



On the periodicity of free oscillations for a finite ice column

Daniel Moreno^{1,2}, Alexander Robinson^{1,2}, Marisa Montoya^{1,2}, and Jorge Alvarez-Solas^{1,2}

¹Departamento de Física de la Tierra y Astrofísica, Universidad Complutense de Madrid, Facultad de Ciencias Físicas, 28040 Madrid, Spain

²Instituto de Geociencias, Consejo Superior de Investigaciones Científicas-Universidad Complutense de Madrid, 28040 Madrid, Spain

Correspondence: Daniel Moreno (danielm@ucm.es)

Abstract. The temperature distribution in ice sheets is worthy of attention given the strong relation with ice dynamics and the intrinsic information about past surface temperature variations. Here we refine the classical analysis of free oscillations in an ice sheet by analytically solving the thermal evolution of an ice column. In so doing, we provide analytical solutions to the one-dimensional Fourier heat equation over a finite motionless ice column for a general boundary condition problem.

5 The time evolution of the temperature profiles appears to be strongly dependent on the column thickness L and largely differs from previous studies that assumed an infinite column thickness. Consequently, the time required for the column base to thaw depends on several factors: the ice column thickness L , the initial temperature profile and the boundary conditions. This timescale is classically considered to be the period of a binge-purge oscillator, a potential mechanism behind the Heinrich Events. Our analytical solutions show a broad range of periods for medium-size column thicknesses. In the limit of $L \rightarrow \infty$,

10 the particular values of the prescribed temperature at the top of the column become irrelevant and the reference value of ~ 7000 years, previously estimated for an idealised infinite domain, is retrieved. More generally, we prove that solutions with different upper boundary conditions, yet covered by our formulation, converge to the same result in such a limit. These results ultimately manifest a subtle connection between internal free and externally-driven (in the sense of a time-dependent boundary condition at the top) mechanisms caused by the finitude of the domain. Thermomechanical instabilities, inherent to internal free

15 oscillations, are in fact sensitive to the particular climatic forcing imposed as a boundary condition at the top of the ice column. Lastly, analytical solutions herein presented are applicable in any context where our general boundary problem is satisfied.

1 Introduction

Periodic episodes of extreme iceberg discharge have captivated the glaciological and paleoclimatological community for the last three decades. Yet the ultimate cause of these so-called Heinrich Events (HE) remains elusive. Several mechanisms have been proposed in the literature that can be broadly classified into two branches: internal free and externally-driven oscillations.



Free oscillations were first proposed in MacAyeal (1993a) as manifestations of the Laurentide Ice Sheet (LIS) purging excess ice volume. This interpretation rests on the assumption that a transition exists between two potential states of basal lubrication (Alley and Whillans, 1991; Hughes, 1992) and it is known as the binge-purge hypothesis. Namely, when the basal ice temperature is below the pressure melting point, the ice sheet is assumed to be stagnant and it simply thickens due to snow accumulation. As a result of the geothermal heat flow, the ice column is expected to warm and the base eventually yields melting. At this point, the ice sheet is no longer at rest and begins to slide over a lubricated sediment bed. MacAyeal (1993a) thus investigated what causes the bed of the LIS in Hudson Bay and Hudson Strait to shift from a frozen to a thawed state as well as the time length involved in this process. To this end, he developed a conceptual model that shows how amplitude and periodicity depend on two environmental factors: the annual average sea-level temperature and the atmospheric lapse rate. Furthermore, a periodicity of $T \approx 7000$ years was estimated from these two factors for a simplified geometry. This value was determined as the time required for the base of a semi-infinite one-dimensional motionless ice column to reach the melting point due to a constant geothermal heat flow (Carslaw and Jaeger, 1988). It is noteworthy the absence of time dependent boundary conditions throughout the study.

Even though both the period and amplitude of the free oscillations appear to be dependent on environmental factors, the same study dismissed the possibility of an oscillation period imposed by an external atmospheric forcing since it would be prohibited by the ice-sheet heat transfer physics. In other words, if such an external climate forcing did exist, its imprint would be strongly attenuated at the base of the ice sheet. In fact, MacAyeal (1993a) showed that the corresponding e -folding decay length of a $T \approx 7000$ years periodicity reads $\sqrt{2k/\omega} = 314$ m for a motionless ice column. Moreover, a constant vertical velocity was also considered, thus increasing the e -folding decay length to 970 m. In view of these results, it is evident that a harmonic surface temperature fluctuation would become negligible at the base of a thick ice sheet.

To provide quantitative support to the conceptual model, a low-order model of the HE cycle was additionally developed (MacAyeal 1993b) to confirm that the theoretical estimation of HE periodicity T is in fact determined by the aforementioned environmental factors. Remarkably, the numerical periodicity showed a discrepancy from the theoretical estimation of solely 4%. However, this relaxation oscillator model assumes a characteristic ice stream purge timescale of 250 years, given the absence of explicit simulations of a Hudson Strait ice stream. Notably, this choice is relevant for the long timescale of the HE since it determines the switch from purge to growth behaviour, found to be 450 years in the numerical results.

Since then, dynamic 3D ice-sheet models have been used to investigate the mechanisms underlying HEs. For instance, Marshall and Clarke (1997) used a 3D model to simulate the LIS, though no discharges were reproduced within the wide range of model parameters. Calov et al. (2002) first modeled oscillatory behaviour in three-dimensional SIA models with *ad hoc* basal sliding. Along with other studies, the authors noted the necessary evolving drainage and till mechanics providing potential insight into our understanding of the physical processes that causes Hudson Strait oscillations (Calov et al., 2002; 2010). Thus, from highly reduced models (e.g., Tulaczyk et al., 2000b) to a complex Herterich-Blatter-Pattyn ice model (e.g., Bougamont et al., 2011), multiple approaches have been found for a wide degree of comprehensiveness in ice stream dynamics in which the basal hydrology has become essential for an appropriate representation of the ice streams.



More recently, Robel et al. (2013) focused on the temporal variability of an ice stream accounting for basal hydrology, modeled as a unique spatial element assuming a single velocity to represent ice discharge. The surface temperature and the geothermal heat flux were found to determine the character of the ice flow. In particular, an oscillatory binge-purge mode was also present and appeared to be primarily caused by re-freezing of meltwater due to ice thinning during stagnation. The remarkable dependence of both the periodicity and the amplitude of these events on the boundary conditions of the system (surface temperature and geothermal heat flux) suggests that even a zero-dimensional spatial model is highly sensitive to time-independent forcing.

Nevertheless, none of these studies discussed the theoretical implications of a HE periodicity estimated under the assumption of a (oversimplified) semi-infinite domain. In addition, these assumptions lack a more general treatment of the plausible boundary conditions at the top of the ice column. Despite the fact that the characteristic binge timescale determined the HE periodicity solely from environmental factors (lapse rate and sea level temperature), it does not necessarily imply that such periodicity is independent of the boundary conditions. Strictly speaking, one can only conclude that the periodicity T cannot be imposed by harmonic forcing.

Even so, the $T \approx 7000$ year periodicity appears widely used in the literature as a reference value for ice-sheet models. Yet the theoretical implications of a more realistic finite medium remain unexplored. We herein investigate the consequences of considering a one-dimensional motionless ice column with a thickness L and quantify the impact of explicit boundary and initial conditions. A formulation of the problem is given in Section 2; the approach followed in this work is presented in Section 3; analytical solutions are shown in Section 4; results are discussed in Section 5 and our concluding remarks are given in Section 6.

2 Finite thickness

Let us now elaborate on the description of a more realistic one-dimensional ice column with a finite thickness L . Our domain is then defined as the interval $y \in [0, L] \equiv \mathcal{L}$. First, we must reformulate the problem imposing the necessary additional boundary condition at the top of the motionless column $y = L$ (Fig. 1).

In the simplest physical scenario, the ice surface temperature is set to the air temperature value $\theta(L, t) = T_{\text{air}}$. However, the particular surface temperature is in fact the result of the energy balance between the ice and the atmosphere. The most general approach considers that the ice and the air may not be always at thermal equilibrium, thus yielding a heat flux due to a vertical temperature gradient. The thermal equilibrium is only reached if the ice surface and the atmosphere temperatures are identical. In such conditions, the heat flux across the interface is null and the vertical gradient at the top the ice column vanishes. As a result, both the surface ice temperature and the vertical gradient can consequently vary in time:

$$\beta \theta_y + \theta = T_{\text{air}}, \quad y = L, \quad t > 0, \quad (1)$$

where β is a parameter with length dimensions and italic subscripts denote partial differentiation.

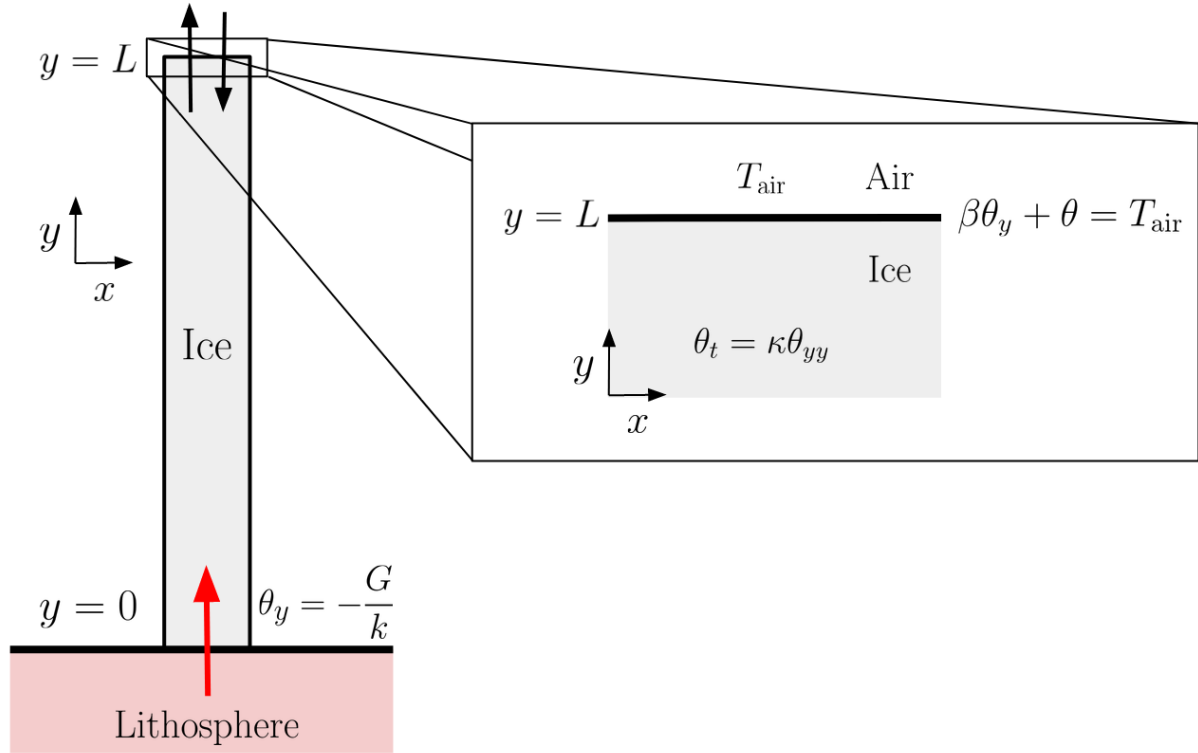


Figure 1. Schematic view of the motionless ice column with a finite thickness L . Subscripts denote partial differentiation. At the top, both the ice temperature and the vertical gradient can vary in time, thus allowing for non-equilibrium thermal states. At the base, the vertical gradient is fixed to the value given by the geothermal heat flux $\theta_y = -G/k$.

The β factor modulates the permissible deviation between ice and air temperatures. In the limit case $\beta = 0$, the interface ice-air is always at thermal equilibrium (i.e., $\theta = T_{\text{air}}$). For $\beta \neq 0$, we allow for a heat exchange across the ice surface driven by the temperature difference between the two media. The ice surface will consequently evolve in time towards T_{air} .

90 Thus, the ice temperature $\theta(y, t)$ satisfies the following initial value problem:

$$\begin{cases} \theta_t = \kappa \theta_{yy}, & y \in \mathcal{L}, t > 0, \\ \theta = \theta_0(y), & y \in \mathcal{L}, t = 0, \\ \theta_y = -G/k, & y = 0, t > 0, \\ \beta \theta_y + \theta = T_{\text{air}}, & y = L, t > 0, \end{cases} \quad (2)$$

where the ice diffusivity is denoted by κ , G is the geothermal heat flux and k is the ice conductivity. The initial temperature profile reads $\theta_0(y) = \theta_b + (\theta_L - \theta_b)y/L$, where θ_L and θ_b are the initial temperature at the top and the base of the column respectively.



95 3 Fourier method

Our aim is to solve the initial value problem by using the Fourier method, also known as separation of variables (an overview of the method is given in Appendix A). Consequently, we first need to find a change of variable that leaves us with homogeneous boundary conditions (e.g., 'shifting the data' technique) in order to determine the corresponding eigenvalues.

Let us then define the new variable $\xi(y, t)$ for the problem determined by the equation Set 2:

$$100 \quad \xi = \theta - T_{\text{air}} + (y - \beta - L) \frac{G}{k} \quad (3)$$

Therefore, in terms of the new variable the problem under consideration reads:

$$\begin{cases} \xi_t = \kappa \xi_{yy}, & y \in \mathcal{L}, t > 0, \\ \xi = f(y), & y \in \mathcal{L}, t = 0, \\ \xi_y = 0, & y = 0, t > 0, \\ \beta \xi_y + \xi = 0, & y = L, t > 0, \end{cases} \quad (4)$$

where $f(y) = \theta_0(y) - T_{\text{air}} + (y - \beta - L) \frac{G}{k}$.

As a result, we now have a homogeneous problem that can be solved by separation of variables (Appendix A). If a solution
 105 exists, it determines the vertical temperature profile at any given time for the initial and boundary conditions provided by the Set 2.

4 Analytical solution

The solution $\xi(y, t)$ to the boundary problem determined by the Set 2 (derivation details in Appendix B) reads:

$$\xi(y, t) = \sum_{n=0}^{\infty} A_n \cos(\sqrt{\lambda_n} y) e^{-\kappa \lambda_n t}, \quad (5)$$

110 where the eigenvalues $\sqrt{\lambda_n}$ are given by the transcendental equation:

$$\tan(L\sqrt{\lambda_n}) = \frac{1}{\beta\sqrt{\lambda_n}}. \quad (6)$$

Equation 6 does not admit an algebraic representation, hence requiring a numerical method to compute λ_n . Here we implemented the Brent-Dekker algorithm (Dekker, 1969; Brent, 1971) with a tolerance of 10^{-8} . This root-finding algorithm choice combines the bisection method, the secant method and the inverse quadratic interpolation.

115 The coefficients A_n can be readily obtained applying orthogonality among eigenfunctions:

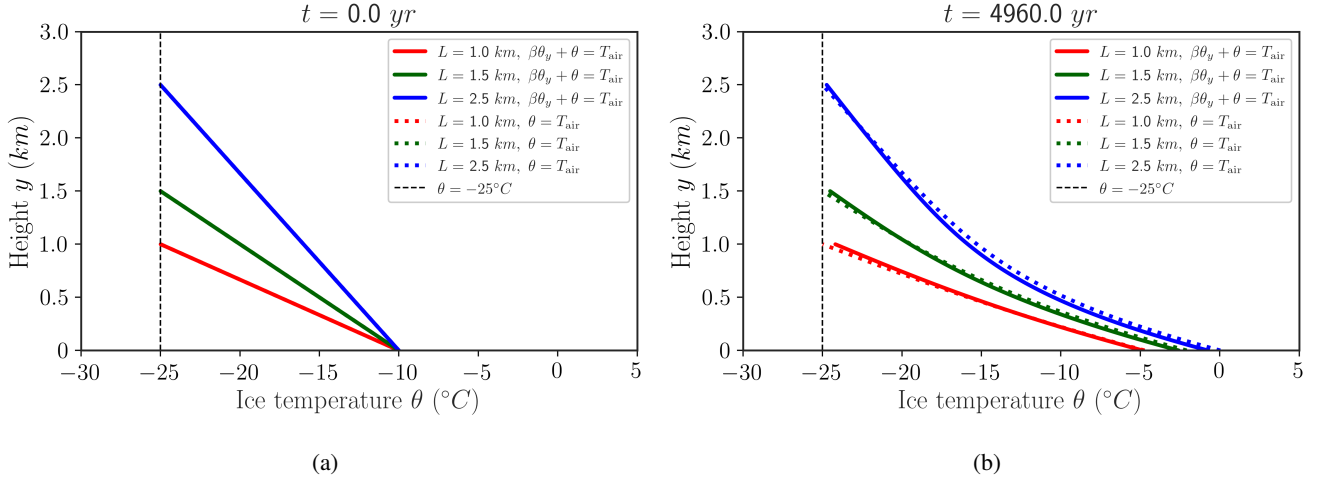


Figure 2. Vertical profiles from analytical solutions $\theta(y, t)$ for three different ice-column thicknesses $L = 1.0, 1.5,$ and 2.5 km. Top panel (a), $t = 0$ yr; bottom (b), $t = 4960$ yr. Solid line represents solutions for $\beta = 50$ m whereas the case $\beta = 0$ is denoted by a dotted line.

$$A_n = \frac{2}{L} \int_0^L \xi(y, 0) \cos(\sqrt{\lambda_n} y) dy. \quad (7)$$

It is noteworthy that if β is strictly zero, the solution is still given by Eq. 5 but Eq. 6 no longer holds (see Appendix C). Rather, the eigenvalues satisfy the equation $\cos(L\sqrt{\lambda_n}) = 0$ and can be obtained analytically as:

$$\sqrt{\lambda_n} = \left(n + \frac{1}{2}\right) \frac{\pi}{L}, \quad (8)$$

120 where $n = 0, 1, 2, \dots$

In this particular case, the corresponding coefficients A_n also allow for analytical expression:

$$A_n = 4(\theta_b - \theta_L) \left[\frac{\cos(n\pi)}{2n\pi + \pi} \right] - 8L \frac{\tilde{G}}{k} \left[\frac{1}{2n\pi + \pi} \right]^2. \quad (9)$$

5 Vertical temperature profile

We now present the vertical profiles $\theta(y, t)$ from analytical solutions given by Eq. 5 for three different thicknesses, $L = 1.0, 1.5$ and 2.5 km, at $t = 0$ and $t = 4960$ years (Fig. 2). The second time frame value is chosen so that the fastest warming scenario precisely reaches melting.

The implications of a finite domain are clear. The lower half of the column warms due to the geothermal heat flux and this rate is in fact proportional to $\sim \kappa \lambda_n e^{-\kappa \lambda_n t}$. Then if we let $L_1 > L_2$, it consequently yields $|\partial\theta_1/\partial t| > |\partial\theta_2/\partial t|$ at $y = 0$. That is, a thicker ice column implies a faster change of its basal temperature.

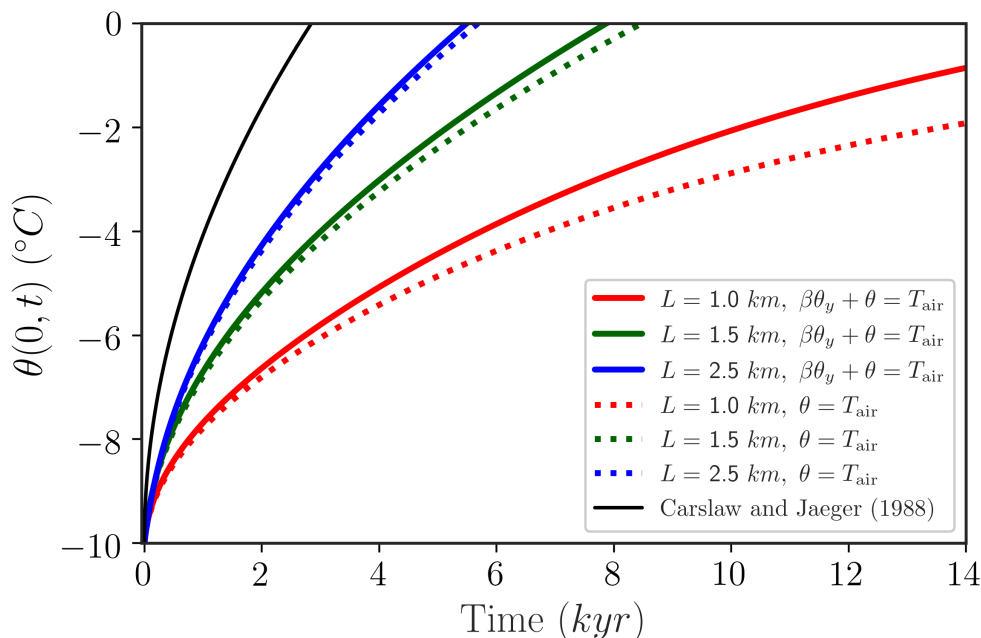


Figure 3. Time evolution of the basal temperature for three different thicknesses. Solid line represents solutions for $\beta = 50$ m whereas the limit case $\beta = 0$ (i.e., fixed surface temperature) is denoted by a dotted line. The boundary condition at the base is identical for all cases and given by the geothermal heat flux G .

130 The impact of β is particularly clear at the top (Fig. 2b), where the temperature slightly increases due to an upward heat flux
 originating at the base (unlike the $\beta = 0$ case where the temperature is prescribed). The specific non-zero β value does not alter
 this behaviour, though larger values yield a greater temperature difference between the ice and the atmosphere. We have chosen
 $\beta = 50$ m to display such mechanism, whilst keeping a reasonable temperature difference (Cuffey and Paterson, 2010). We can
 then physically interpret this parameter as the thermal insulation of the ice-air interface. Thus, a zero value corresponds to an
 135 ideal conductor ($\theta(L, t) = T_{\text{air}}$), whereas $\beta \rightarrow \infty$ represents a perfect thermal insulator characterized by a null heat exchange
 across the interface.

6 A new period for the binge/purge oscillator

First, we present the temporal dependency of the basal temperature (Fig. 3) from our analytical solution (Eq. 5). We further
 calculate the time required for the column base to reach the melting point analogously to the growth phase of a Heinrich event
 140 oscillation (MacAyeal, 1993a), hereinafter referred as potential periodicity (Fig. 4).

Figure 3 shows the sensitivity of the thermal state of the base to the thickness of the column L and to the mathematical
 treatment of the surface boundary condition. It is clear that the column thickness is the primary factor that allows the surface



temperature to influence the evolution of the base. Strictly speaking, the external forcing perturbs the temperature vertical profile of the ice column, thus determining the basal temperature. When we allow for non-equilibrium thermal states in the top boundary condition (i.e., $\beta \neq 0$), the base warms faster since the column surface can evolve in time towards higher temperatures, thus inducing a lower temperature difference between the base and the top. The relevance of such effect is quantified by the column thickness, becoming negligible for large L values.

For a fixed β and a particular initial state, the rate of change of the basal temperature solely depends on the column thickness L , the choice of G and T_{air} . Nevertheless, when computing the time required for the base to thaw, the initial temperature profile plays an essential role.

Figure 4 shows the dependency of the potential periodicity on both the initial and boundary conditions in our general formulation (Eq. 1). The impact of the external forcing is evident from Fig. 4b. As we would expect, lower T_{air} values yield longer potential periods, though solely for ice thicknesses below ~ 2 km. Otherwise, the periodicity appears to be independent of the surface ice temperature. We therefore find that $L = 2$ km is a threshold value, above which the periodicity is decoupled of the top boundary condition.

The potential periodicity decreases as the geothermal heat flux increases. A similar behaviour is found with increasing L due to the thermal insulating effect of the ice column, particularly for low geothermal heat flux values.

The initial conditions are also essential to quantify the time required for the ice base to thaw. We have considered a linear initial vertical profile $\theta_0(y) = \theta_b + (\theta_L - \theta_b)y/L$, so as to understand the explicit dependency of the initial surface temperature θ_L and the initial basal temperature θ_b independently (Figs. 4c and 4d). Namely, the impact of θ_L is determined by the column thickness, with a more acute dependence for low L values. Lastly, the potential periodicity appears to be rather sensitive to the initial basal temperature, rapidly saturating to values above 25 kyr for $\theta_b < -11^\circ\text{C}$.

7 The limit $L \rightarrow \infty$

Compared to previous work, the analytical solutions presented herein account for an additional degree of freedom in terms of the domain definition: the ice column thickness L . Nonetheless, this solutions should converge under certain conditions to the L -independent solution of Carslaw and Jaeger (1988) if we let $L \rightarrow \infty$. For completeness, we shall show that the theoretical periodicity of MacAyeal (1993a) is in fact retrieved in such limit irrespective of the specific boundary condition at the top.

The particular conditions under which our solution converge must imply an equivalent physical scenario to the one established by MacAyeal (1993a). Specifically, he considered an initial temperature profile that follows an atmospheric lapse rate Γ since the ice column is assumed to be assembled by snow precipitation. Hence the temperature solution is decomposed into a steady and a transient component, corresponding to Γ and the 'excess' of geothermal heat flux $\tilde{G} = G - k\Gamma$ respectively. If we account for this particular formulation in our more general approach, the estimated 6944-year-period is retrieved in the limit $L \rightarrow \infty$ (Fig. 5).

Even though the eigenvalues of our problem satisfy a different relation in the limit $\beta = 0$, we shall prove that convergence to the 6944-year-period is independent of β and therefore consistent with previous results. Let φ and ϕ be two solutions of

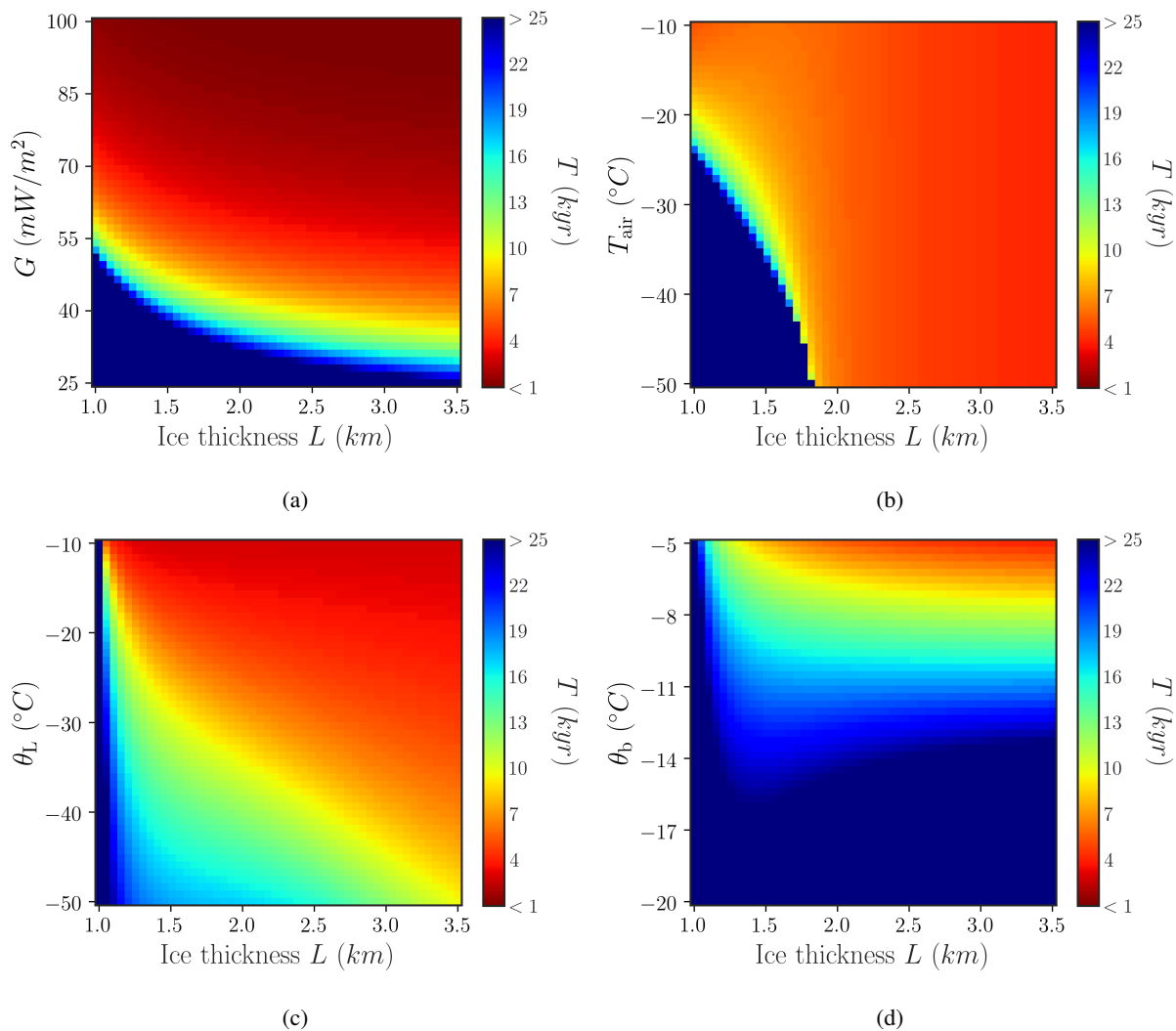


Figure 4. Potential periodicity T as a function of the ice thickness L , initial and boundary conditions in our general formulation. $\beta = 50$ m for all solutions. (Eq. 1). Boundary conditions: (a) Geothermal heat flux G and (b) Air temperature T_{air} . Initial conditions: (c) Initial ice surface temperature θ_L and (d) Initial basal temperature θ_b .



our general boundary problem (Set 2) with a zero and a non-zero β value respectively and arbitrary initial conditions. The difference between solutions is then:

$$\Delta \doteq \phi - \varphi = \sum_{n=0}^{\infty} \left[A_n \cos(\sqrt{\lambda_n} y) e^{-\kappa \lambda_n t} - \tilde{A}_n \cos(\sqrt{\tilde{\lambda}_n} y) e^{-\kappa \tilde{\lambda}_n t} \right]. \quad (10)$$

We must recall that the eigenvalues for a non-zero β case (i.e., ϕ) must satisfy Eq. 6. With an appropriate change of variable
 180 $x_n = L\sqrt{\lambda_n}$, it is clear that:

$$\lim_{L \rightarrow \infty} \left[\tan(x_n) = \frac{L}{\beta x_n} \right] \rightarrow x_n = \left(n + \frac{1}{2} \right) \pi, \quad (11)$$

where $n = 0, 1, 2, \dots$, which precisely correspond to the eigenvalues of the $\beta = 0$ case.

Hence, it is straightforward that the spatial and temporal dependency in Δ vanish in the limit $L \rightarrow \infty$. Additionally, given that the only L -order term is not proportional to β in the initial conditions, the coefficients A_n and \tilde{A}_n become identical in such
 185 a limit. We then conclude that $\Delta = 0$ if β is finite as $L \rightarrow \infty$. In other words, we have proven that both solutions are identical irrespective of β as the ice thickness approaches infinity.

MacAyeal (1993a) seemingly showed that the boundary conditions and the ice base temperature are decoupled by estimating that the e -fold decay of a periodic forcing with $\omega = 2.84 \times 10^{-11} \text{ s}^{-1}$ in a motionless column reads $\sqrt{2k/\omega} = 314 \text{ m}$. This estimation solely considers periodic signals, whilst leaving unexplored the implication of a non-periodic forcing. Our results
 190 affirm otherwise: though an oscillatory forcing rapidly attenuates with depth, Fig. 4 and 5 show that the base is in fact strongly coupled with both the external conditions and the initial thermal state of the ice. The strength of this coupling is determined by the column thickness L .

8 Conclusions

We have considered the implications of a finite one-dimensional ice column domain with a given thickness L on the solutions
 195 of Fourier heat equation. Unlike previous work, we provide analytical solutions that are explicitly dependent on this new degree of freedom, thus quantifying its relevance without further approximations.

As a result of our new domain extension, we have studied physically-plausible scenarios imposed by a general boundary condition at the top of the motionless ice column. This approach considers that the ice and the air may not be always at thermal equilibrium, thus yielding a heat flux across the interface due to a vertical temperature gradient. As a result, both
 200 the ice temperature at the top and its vertical gradient are allowed to vary in time. If the ice surface happens to reach the air temperature, the vertical gradient vanishes leading to a thermal equilibrium state.

We find that the ice thickness plays a fundamental role in the Fourier solutions, which implies that a semi-infinite domain is an oversimplification. The temperature at the base is highly dependent on the particular boundary condition at the top of the ice column. Particularly, these solutions are significantly distinct from each other for ice thicknesses $L < 2 \text{ km}$.

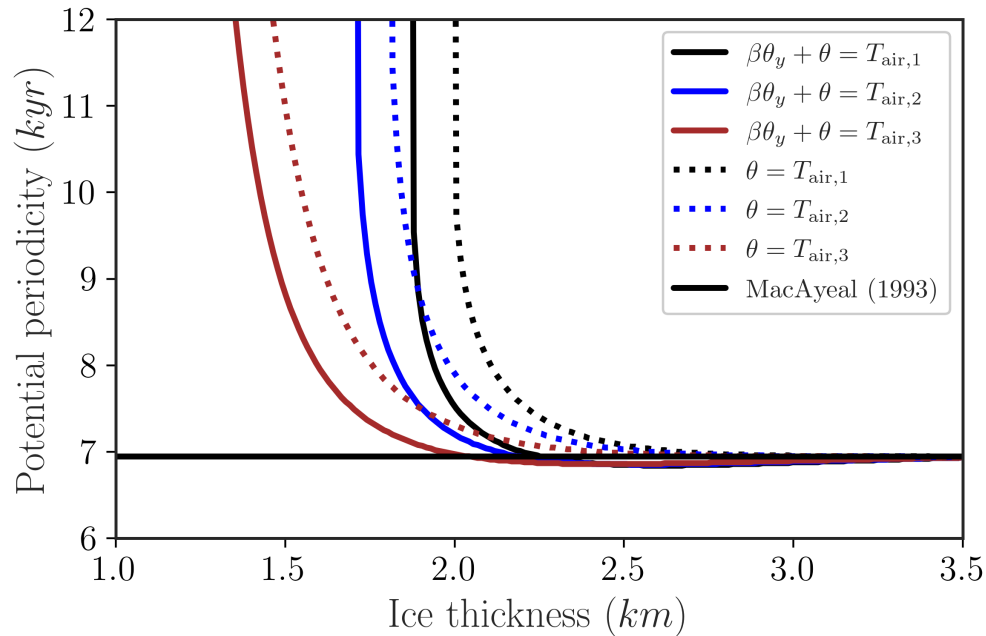


Figure 5. Time required for the column base to thaw as a function of the ice column thickness L , allowing us to define a potential Heinrich Event periodicity from analytical solutions. Colour represents the air temperature: $T_{\text{air},1} = -40^\circ\text{C}$, $T_{\text{air},2} = -30^\circ\text{C}$ and $T_{\text{air},3} = -20^\circ\text{C}$. Solid line represents solutions for $\beta = 50$ m whereas the case $\beta = 0$ (i.e., fixed surface temperature) is denoted by a dotted line. The boundary condition at the base $\theta_y = -\tilde{G}/k$ is identical for all cases.

205 Our analytical approach allows us to quantify the sensitivity of the solution to the initial and boundary conditions. In particular, the thermal state of the base completely decouples from the upper boundary condition (i.e., external forcing) for L values above 2 km and its thermal evolution becomes solely a function of the lower boundary condition (i.e., the geothermal heat flux).

Notably, in the limit $L \rightarrow \infty$, the prior L -independent solution (Carslaw and Jaeger, 1988) is retrieved, consequently yielding
 210 the 6944 years periodicity estimated by MacAyeal (1993a). For completeness, we showed that such periodicity is in fact retrieved irrespective of the particular boundary condition at the top. This confirms the robustness of our results.

Regarding a potential estimation of the binge-purge periodicity based on our analytical solutions, the new degree of freedom L entails strong consequences. First, large temporal variability can be explained solely by considering a change in ice thickness without any additional factors. In other words, this provides a source of natural internal variability irrespective of the external
 215 forcing. For medium-size ice sheets, this variability spans a 7-12 kyr range. In addition, the explicit consideration of distinct initial temperature profiles manifests a high sensitivity of the binge-purge oscillator period to its initial state.

Moreover, a finite thickness also determines the mechanism by which an atmospheric perturbation might potentially influence the time required to melt the ice base since we have quantified the effect of a prescribed surface temperature and a vertical



220 gradient. For a fixed L value, besides the geothermal heat flux, both the vertical gradient and the temperature at the top govern the temperature time evolution, consequently defining the particular binge-purge periodicity estimation.

It must be stressed that, even though we have shown that the ice base temperature is in fact coupled with the boundary conditions, the periodicity of such events cannot be imposed by the frequency of an external forcing. Rather, the potential period of the oscillator is determined by the ice thickness and the energy condition at the base and the surface.

225 Lastly, we note that a subtle connection exists between internal free and externally-driven (in the sense of a time-dependent boundary condition at the top) mechanisms caused by the finitude of the domain. Thermomechanical instabilities, inherent to internal free oscillations, are in fact sensitive to the particular climatic forcing imposed as a boundary condition at the top of the ice column. This double-fold nature of thermomechanical instabilities is only exhibited when a finite domain is considered, further supporting the use of such analytical solutions in simple low-dimensional ice-sheet models where temperature profiles are otherwise prescribed.

235 **Appendix A: Separation of variables**

Let us briefly outline the separation of variables technique before elaborating on the solutions of our general problem. Consider the following initial/boundary problem on an interval $\mathcal{I} \subset \mathbb{R}$,

$$\begin{cases} u_t = \kappa u_{yy} & y \in \mathcal{I}, t > 0 \\ u(y, 0) = \varphi(y) & y \in \mathcal{I} \\ u \text{ satisfies certain BCs.} \end{cases} \quad (\text{A.1})$$



This technique looks for a solution of the form:

$$240 \quad u(y, t) = Y(y)T(t), \tag{A.2}$$

where the functions Y and T are to be determined. Assuming that there exists a solution of A.1 and plugging the function $u = YT$ into the heat equation, it follows:

$$\frac{T'}{\kappa T} = \frac{Y''}{Y} = -\lambda, \tag{A.3}$$

for some constant λ . Thus, the solution $u(y, t) = Y(y)T(t)$ of the heat equation must satisfy these equations. Additionally, in
245 order for u to satisfy the boundary conditions, we arrive to:

$$\begin{cases} Y''(y) = -\lambda Y(y) & y \in \mathcal{I} \\ Y \text{ satisfies our BCs.} \end{cases} \tag{A.4}$$

This is a well-known eigenvalue problem. Namely, a constant λ that satisfies Eq. A.4 for some function X (not identically zero) is called an eigenvalue of $-\partial_y^2$ for the given boundary conditions. Hence, the function Y is an eigenfunction with associated eigenvalue λ .

250 Therefore, in order for a function of the form $u(y, t) = Y(y)T(t)$ to be a solution of the heat equation on the interval $\mathcal{I} \subset \mathbb{R}$, T must be a solution of the ODE $T' = -\kappa\lambda T$. Direct integration leads to:

$$T(t) = Ae^{-\kappa\lambda t}, \tag{A.5}$$

for an arbitrary constant A . Thus, for each eigenfunction Y_n with corresponding eigenvalue λ_n , we have a solution T_n such that:

$$255 \quad u_n(y, t) = Y_n(y)T_n(t), \tag{A.6}$$

is a solution of the heat equation on our interval \mathcal{I} which satisfies the BC. Moreover, given that the problem A.1 is linear, any finite linear combination of a sequence of solutions $\{u_n\}$ is also a solution. In fact, it can be shown that an infinite series of the form:

$$u(y, t) \equiv \sum_{n=1}^{\infty} u_n(y, t), \tag{A.7}$$

260 will also be a solution of the heat equation on the interval \mathcal{I} that satisfies our BC, under proper convergence assumptions of this series. The discussion of this issue is beyond the scope of this work.



Appendix B: Solution of the problem

Let us elaborate on the solution of our general problem (Section 4) by first solving the associated eigenvalue problem. As we employ the separation of variables technique, the solution takes the form:

$$265 \quad \xi(y, t) = \sum_{n=0}^{\infty} Y_n(y) T_n(t), \quad (\text{B.1})$$

where the functions $Y_n(y)$ and $T_n(t)$ are to be determined. After the consequent change of variable so that $Y(y)$ satisfies Eq. A.4, we arrive to:

$$Y_n(y) = A_n \cos(\sqrt{\lambda_n} y) + B_n \sin(\sqrt{\lambda_n} y), \quad (\text{B.2})$$

where A_n and B_n are to be determined. Applying the boundary conditions imposed in Set 2, it is clear that all sine coefficients
 270 are identically zero $B_n = 0$ and the eigenvalues $\sqrt{\lambda_n}$ are given by the transcendental equation:

$$\tan(L\sqrt{\lambda_n}) = \frac{1}{\beta\sqrt{\lambda_n}}, \quad (\text{B.3})$$

that admits no algebraic representation, hence requiring a numerical method to compute λ_n .

From orthogonality of the eigenfunctions $Y_n(y)$, the coefficients A_n of our solution are calculated following:

$$A_n = \frac{2}{L} \int_0^L \xi(y, 0) \cos(\sqrt{\lambda_n} y) dy. \quad (\text{B.4})$$

275 where $\xi(y, 0) = \frac{\tilde{C}}{k} (y - L) - \theta_L + \theta_b$. Even though $\xi(y, 0)$ is a function of the form $f(y) = ay + b$, the integration of the coefficients A_n does not yield analytical representation since the eigenvalue equation is transcendental.

Hence, the solution of our general problem reads:

$$\xi(y, t) = \sum_{n=0}^{\infty} A_n \cos(\sqrt{\lambda_n} y) e^{-\kappa\lambda_n t}, \quad (\text{B.5})$$

Appendix C: Limit case $\beta = 0$

280 It is crucial to consider that the eigenvalue equation given by Eq. 6 does not hold for $\beta = 0$. In such case, after the consequent change of variable so that $Y(y)$ satisfies Eq. A.4, we arrive to:

$$Y_n(y) = A_n \cos(\sqrt{\lambda_n} y) + B_n \sin(\sqrt{\lambda_n} y), \quad (\text{C.1})$$



where A_n and B_n are to be determined. Applying the boundary conditions imposed in Set 2, it is clear that all sine coefficients are identically zero, $B_n = 0$, and the eigenvalues read:

$$285 \quad \sqrt{\lambda_n} = \left(n + \frac{1}{2}\right) \frac{\pi}{L}, \quad (\text{C.2})$$

where $n = 0, 1, 2, \dots$

From orthogonality of the eigenfunctions $Y_n(y)$, the coefficients A_n of our solution are calculated following:

$$A_n = \frac{2}{L} \int_0^L \xi(y, 0) \cos(\sqrt{\lambda_n} y) dy. \quad (\text{C.3})$$

where $\xi(y, 0) = \frac{\tilde{G}}{k} (y - L) - \theta_L + \theta_b$. Since $\xi(y, 0)$ is a function of the form $f(y) = ay + b$ and the eigenvalues allow for an
 290 analytical expression, the integration of the coefficients A_n is straightforward:

$$A_n = 4(\theta_b - \theta_L) \left[\frac{\cos(n\pi)}{2n\pi + \pi} \right] - 8L \frac{\tilde{G}}{k} \left[\frac{1}{2n\pi + \pi} \right]^2. \quad (\text{C.4})$$

It is clear that this series converges and satisfies the initial condition imposed by $\xi(y, 0)$ given that:

$$\sum_{n=0}^{\infty} \frac{\cos(n\pi)}{2n\pi + \pi} = \frac{1}{4}, \quad (\text{C.5a})$$

$$\sum_{n=0}^{\infty} \frac{1}{(2n\pi + \pi)^2} = \frac{1}{8}. \quad (\text{C.5b})$$

295 Hence, the solution of Problem 1 reads:

$$\zeta(y, t) = \sum_{n=0}^{\infty} A_n \cos(\sqrt{\lambda_n} y) e^{-\kappa \lambda_n t}, \quad (\text{C.6})$$

Author contributions. Daniel Moreno formulated the problem, derived the analytical solutions, analysed the results and wrote the paper. All other authors contributed to analyse the results and writing the paper.

300 *Competing interests.* Alexander Robinson is an editor of The Cryosphere. The peer-review process was guided by an independent editor, and the authors have also no other competing interests to declare.



Acknowledgements. Daniel Moreno, Alexander Robinson and Jorge Alvarez-Solas were supported by the Spanish Ministry of Science and Innovation project ICEAGE (grant no. PID2019-110714RA-100). Alexander Robinson was also supported by the Ramón y Cajal Programme of the Spanish Ministry for Science, Innovation and Universities (grant no. RYC-2016-20587).



References

- Alley, R. and Whillans, I.: Changes in the West Antarctic ice sheet, *Science*, 254, 959, 1991.
- Bougamont, M., Price, S., Christoffersen, P., and Payne, A. J.: Dynamic patterns of ice stream flow in a 3-D higher-order ice sheet model with plastic bed and simplified hydrology, *Journal of Geophysical Research*, 116, <https://doi.org/10.1029/2011jg002025>, 2011.
- 310 Brent, R.: Brent, Richard P. An algorithm with guaranteed convergence for finding a zero of a function., *The computer journal*, 14, 422–425, 1971.
- Calov, R., Ganopolski, A., Petoukhov, V., Claussen, M., and Greve, R.: Large-scale instabilities of the Laurentide ice sheet simulated in a fully coupled climate-system model, *Geophysical Research Letters*, 29, 69–1, 2002.
- Calov, R., Greve, R., Abe-Ouchi, A., Bueller, E., Huybrechts, P., Johnson, J. V., Pattyn, F., Pollard, D., Ritz, C., Saito, F., and Tarasov, L.:
315 Results from the Ice-Sheet Model Intercomparison Project–Heinrich Event Intercomparison (ISMIP HEINO), *Journal of Glaciology*, 56, 371–383, <https://doi.org/10.3189/002214310792447789>, 2010.
- Carslaw, H. S. and Jaeger, J. C.: *Conduction of heat in solids*, Clarendon Press, Oxford, 1988.
- Cuffey, K. M. and Paterson, W. S. B.: *The Physics of Glaciers*, ACADEMIC PR INC, https://www.ebook.de/de/product/10550595/kurt_m_cuffey_w_s_b_paterson_the_physics_of_glaciers.html, 2010.
- 320 Dekker, T.: Finding a zero by means of successive linear interpolation., *Constructive Aspects of the Fundamental Theorem of Algebra*, B. Dejon and P. Henrici, Eds., Wiley Interscience, London, 1969.
- Hughes, T.: On the pulling power of ice streams, *Journal of Glaciology*, 38, 125–151, <https://doi.org/10.3189/s0022143000009667>, 1992.
- MacAyeal, D. R.: Binge/purge oscillations of the Laurentide ice sheet as a cause of the North Atlantic’s Heinrich events, *Paleoceanography*, 8, 775–784, 1993a.
- 325 MacAyeal, D. R.: A low-order model of the Heinrich event cycle, *Paleoceanography*, 8, 767–773, 1993b.
- Marshall, S. and Clarke, G.: A continuum mixture model of ice stream thermomechanics in the Laurentide Ice Sheet 2. Application to the Hudson Strait Ice Stream, *Journal of Geophysical Research*, 102, 20 615–20, 1997.
- Robel, A. A., DeGiuli, E., Schoof, C., and Tziperman, E.: Dynamics of ice stream temporal variability: Modes, scales, and hysteresis, *Journal of Geophysical Research: Earth Surface*, 118, 925–936, <https://doi.org/10.1002/jgrf.20072>, 2013.
- 330 Tulaczyk, S., Kamb, W. B., and Engelhardt, H. F.: Basal mechanics of Ice Stream B, west Antarctica: 2. Undrained plastic bed model, *Journal of Geophysical Research: Solid Earth*, 105, 483–494, <https://doi.org/10.1029/1999jb900328>, 2000b.